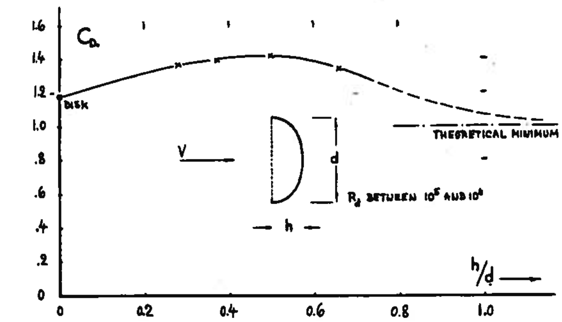

Fig. 31. Drag coefficient of sheet-metal "caps" (40,a) as a function of their height ratio.

Caps and Cups. As large as the drag coefficients of plates may be, there are other shapes exhibiting still higher values. Figure 31 shows the drag coefficient of open cup- or cap-like bodies (similar to parachute canopies). The maximum drag coefficient (on projected area) is obtained for h/d in the order of 0.5, a shape which is ≈ hemispherical. Upon further increasing the height ratio, the rear side more and more changes into a wake "fairing". The drag coefficient is, therefore, expected to approach the theoretical minimum which corresponds to full stagnation pressure across the opening.

7. DRAG OF WEDGES AND CONES

Figures 32 and 33 present shape and drag coefficient of a number of three- and two-dimensional bodies. All of these shapes have a more or less separated flow pattern; most of them have negative pressure on their rear side; and their drag coefficients are comparatively high.

Angle of Flow. To establish some order in the drag coefficients of various shapes, the geometrical angle is very useful, at which the flow is guided by the body's surface upon separating from its rear side. The flat plate, for example, has such an angle "ε" = 90°. A "fold" with a vertex angle of two times 45°, has a separation angle of 90° plus or minus 45°, depending upon the direction of the oncoming flow. Figure 34 demonstrates how the drag coefficient increases as a function of the shape angle. Two branches are found, of course; one for two-dimensional bodies (between walls) and another one for three-dimensional conditions. At "ε" = 0, parallel-sided round-nosed shapes have been used in the graph; a hallow, scoop-like body is plotted at 180°.

Figure 32 (near). Drag coefficients of various 3-dimensional bodies (40) at R'numbers between 10^4 and 10^6. Note: (•) tested on wind-tunnel floor.

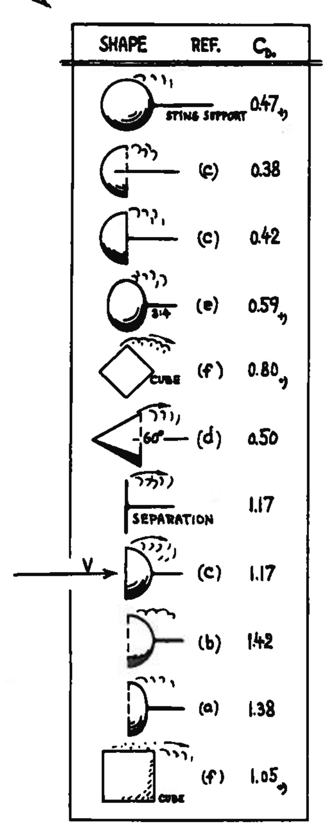

Figure 33 (right). Drag coefficients (41) of 2-dimensional shapes (between walls) at R between 10^4 and 10^6. Note: (+) in subcritical flow.

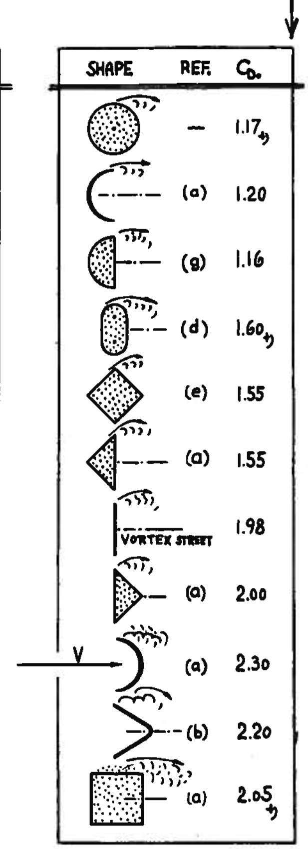

¶ (37) Information on rear-side pressure of plates:
a) On disks and small-aspect-ratio plates see: NACA (36, a); AVA Ergebnisse IV; reference (40,f).
b) On plates between walls see: (12), (35,a) and (40,f).
¶ (40) Experimental results on three-dimensional bodies:
a) Doetsch, Parachute Models, Lufo 1938 p.577.
b) NACA, Cup Anemometer, Tech Rpt 513 (1935).
c) AVA, Hemispherical Bodies, Ergebnisse IV (1932).
d) Eiffel, Recherches a Tour Eiffel, Paris 1907.
e) Hemispherical Cup at $R_d = 2\ 10^5$, ARC RM 712 (1919).
f) Irminger and Nokkentved, Elementary Bodies and Buildings, Kopenhagen 1930 and 1936; Transl'n by Jarvis.
¶ (41) Sections (tested between plates or walls):
a) Lindsey, Simple Shapes, NACA T. Rpt 619 (1940).
b) Junkers Wind-Tunnel, Report Ströte V.9609 (1940).
c) Interference Between Struts, NACA T. Rpt 468 (1933).
d) Delany-Sorensen, Various Shapes, NACA T.Note 3038.
e) AVA Göttingen, Ergebnisse II (1923) and III (1926).
f) Junkers Wind-Tunnel Result on Angle Profile.
g) Reported by Barth, Zt.Flugwissen 1954 p.309.
¶ (42) Free-streamline (cavitation) theory:
a) Kirchhoff, Free Jet Theory, Crelle 1869 (see Lamb).
b) Bobyleff, Russian Phys.-Chem. Society 1881 (see Lamb).
c) Riabouchinsky-Plesset-Schafer, Journal Appl.Physics 1948 p.934, and Review Modern Physics 1948 p.228.
d) Reichardt, Laws of Cavities, German ZWB UM 6628.
¶ (43) Neef, Dive Brakes, Fieseler Tunnel Rpt 22 (1941).